Bulletin of Faculty of Science, Zagazig University (BFSZU)
e-ISSN: 1110-1555
Volume-2023, Issue-3, pp-66-76
https://bfszu.journals.ekb.eg/journal
Research Paper DOI: **10.21608/bfszu.2023.185066.1240**

==========

Using eco-friendly glass from rice straw ash as a shield for cosmic rays

K.R.M. Abdelgawad[1], G.S.M. Ahmed[2], A.T.M. Farag[2], A.A. Bendary[2], S.M. Salem[2], B.A. Tartor[1], I.I. Bashter[1]

[1]Physics Department, Faculty of Science, Zagazig University, Zagazig, Egypt
[2]Physics Department, Faculty of Science, Al-Azhar University, Cairo, Egypt
Corresponding author: karrimanegy37@gmail.com

***ABSTRACT*: Cosmic radiation one of the most important challenges scientists have to deal with due to further developing in the space travel. High-energy particles have a bad effect not only on human beings but also on electronics even in microsatellites or unique unmanned spacecraft. The purpose of this work was to investigate particles found in cosmic radiation and how to decrease its impact on organic and inanimate matter. We provide a new developed (Bi_2O_3-B_2O_3) glass system incorporated with silica from rice straw ash (RSA) with composition equation{(70-x) [$80SiO_2 – 20B_2O_3$]- $30Na_2O$ – x Bi_2O_3}, where x:(0, 5, 10, 15, 20), and explain why this glass can assist protective spaceships or satellites from cosmic radiation by studying glass samples ability to block gamma rays, protons and alpha particles. The purity and chemical composition of the silica are determined using XRF. In addition, WINXCOM software is used theoretically to calculate the shielding parameters like linear attenuation coefficient, half value layer, mean free path and the effective atomic number across a broad range of gamma-ray energies (0.1- 15 MeV). The ion distribution and ionization within glass samples were tracked using TRIM software.**

KEYWORDS: cosmic rays; high energy interactions; radiation protection; LAC; Zeff.

Date of Submission: 02-01-2023 Date of acceptance: 13-03-2023

I. INTRODUCTION

Cosmic radiation is one of the most important challenges scientists have to deal with due to further developing space travel. Understanding the nature of the space radiation environment and how radiation risks influence mission planning, timelines and operational decisions. Exposure to space radiation can create errors in electronics or react with nuclei in the human body which increases the risks of astronauts developing cancer, experiencing central nervous system (CNS) decrements, exhibiting degenerative tissue effects or developing acute radiation syndrome. One or more of these deleterious health effects could develop during future multi-year space exploration missions beyond low Earth orbit (LEO). The primary cosmic rays, which are produced directly through processes in space, mostly consist of protons (89%), alpha particles (9%), and other bare nuclei of atoms (1%), as well as a few electrons (i.e., beta particles, 1%). Cosmic rays with high atomic number and energy, also called HZE (High Z and Energy) ions, make up only approximately 1% of the galactic cosmic rays, but due to their high energy and the high charge of these ions, they are as dangerous as the much more frequently occurring protons. Glass has alternative and promising radiation shielding properties. These unique properties are resulted from their high flexibility of composition, ease of fabrication, high thermal stability, high dielectric constant and low crystallization ability **(Sayyed et al., 2018a; Singh et al., 2003; Sayyed, 2016a, 2016b)**. Due to easily fabrication and excellent transparency to the visible light. The silicate glass is the most commonly commercial glass **(Kaur et al., 2016; Sayyed et al., 2021)**. We extract silica from rice straw ash to reduce both environmental impact and cost of glass production as the main element of rice straw ash is silica where it contains about 62-82% silica **(Tuscharoen et al., 2012; Ruengsri et al., 2015)**. In the present work, Bi_2O_3-B_2O_3 RSA glass has been considered. The structural changes induced in ternary bismuth borate RSA glass when SiO_2 replaces Bi_2O_3 content. The TRIM (transport of ions in matter) package was also used to discover the emptiness distribution and

ionization resulting from the energy loss due to penetration of alpha and proton inside the prepared glass. These effects supply a technical image of the developed interactions and a quantification of the radiation defects. The aim of the present study is the fabrication of eco-friendly Bi_2O_3- B_2O_3- RSA glass using rice straw ash as a silica source and using it as shield of cosmic radiation.

II. MATERIALS AND METHODS

2.1. Sample preparation: Rice straw (RS) was provided from Zagazig, Egypt and treated by ethyl alcohol and tab water boiled for 1.5 h. after that, washed with tab water. The residue was filtered and dried in an oven at 100 ^oC for 1 h. the obtained RS was fed into 3 N HCL solutions in tab water and boiled for 1.5 h. then, the residue was filtered again after washing with tab water and dried in an oven at 100 ^oC for 1 h. Finally, the treated RS placed in a porcelain crucible and loaded into the furnace at 750 ^oC for 2 h to the RSA. Glass samples were prepared using confidential melt and quenching technique considered as $\{(70\text{-}x)\ [80SiO_2 - 20B_2O_3] - 30Na_2O - x\ Bi_2O_3\}$, where x is expressed in terms of mol% (x=0, 5, 10, 15, 20). The mixture was grinding in a gate mortar and transferred into a porcelain crucible. The batches were melt in an electric furnace at 1200oC for 2 h. Accordingly, five different glass compositions were prepared and coded as indicated in table (2).

2.2. Glass characterization: The extracted RSA (SiO_2) was analyzed by X- ray fluorescence (XRF) using PANalytical Axios advanced. Where the amorphous nature of the prepared glasses were examined using X-ray diffractometer (XRD, Shimadzu), with K-Alpha (1.5406 Å) and generator settings 40 KV, 40 mA through standard scanning range of 2Θ from 10^o to 80^o

The densities of the prepared samples were quantified at room temperature by applying Archimedes method using toluene solution (0.87 g/cm^3) as immersion liquid using the following formula,

$$\rho = \left(\frac{m_a}{m_a - m_l}\right)\rho_l \qquad (1)$$

Where ma, ml and ρl are weights of samples in air, liquid and liquid density, respectively.

The molar volume (Vm) of the glass sample was calculated using the following equation,

$$V_m = \frac{\sum_i X_i M_i}{\rho} \qquad (2)$$

Where ρ is the glass sample density and Xi, Mi are the mole fraction and molecular weight of ith oxides, respectively.A carelzeiss-PMQ spectrometer has been used for measuring the transmission spectra and evaluates the optical parameters. The measurements were carried-out at room temperature in the spectral range from 190 to 1100 nm. Deuterium pomp in the range 285-325 nm was used as a source for shorter wavelength and a tungsten lamp in the range 325-2500 nm was used in the visible and near infrared regions.

2.3. Radiation Shielding Properties: The Beer-Lambert law was used to calculate the linear attenuation coefficient (LAC) values, which are given by the following equation **(Kassem et al., 2021)**;

$$I = I_0 e^{-(LAC)x} \qquad (3)$$

where I_0 and I are the incident and transmitted photon beam intensities respectively. x (cm) is the thickness of the sample **(ASKIN, 2020)**. For all elements in a given energy zone, LAC is roughly the same. The mean distance traveled by a photon inside the shielding material before being interacted is the photon mean free path (MFP) **(ALMisned et al., 2021)** and can be calculated using the value of the LAC as the following.

$$\mathrm{MFP} = \frac{1}{\mathrm{LAC}} \qquad (4)$$

The LAC may be used to calculate the half-thickness, which is the thickness of the material sample necessary to reduce the photon beam intensity to half of its original value, as shown in the following equation **(Kaewkhao et al., 2008; VERMANI and SINGH, 2021; Sayyed et al., 2018b)**,

$$HVL = \frac{0.693}{\mathrm{LAC}} \qquad (5)$$

Materials with a high atomic number are regarded as good radiation absorbers because elements with high Z values have greater radiation shielding characteristics **(CENGIZa and ÇAGLAR, 2020)**. In the case of the compound, a Z_{eff} for the composition elements is obtained. The Z_{eff} stands for the material's weighted average atomic number, which is directly proportional to total atomic and electronic cross-sections via the formula below;

$$Z_{eff} = \frac{\sigma_{(t,a)}}{\sigma_{(t,el)}} \qquad (6)$$

where σ (t, a) and σ (t, el) are defined as the probability of mono-energetic photons colliding with atoms and electrons inside this substance during any energy level. The Z_{eff} is not constant, it varies with the material

composition and the incident photon energy, and it provides vital information about the material used for radiation protection **(ALMisned et al., 2021)**.
The TRIM theoretical simulations were also used to explore the vacancy distribution and ionization resulting from the energy loss due to both penetrating alpha and proton ions and recoil atoms inside the glass samples.
These results give a technical image of the developed interactions and a quantification of the radiation defects.

III. RESULTS

The XRF results exhibited the chemical composition of the RSA as shown in table (1). It was seen that the extracted silica reached 98.6%. The density and molar volume of the prepared glasses with different Bi_2O_3 content are given in table (2), where the replacement of Bi_2O_3 at the expense of all SiO_2 and B_2O_3 leads to density growth from 2.373 to 4.076 g/cm3.

Table (1): the XRF analysis in wt % and Chemical constituents of RSA.

Constituents Wt%	SiO_2	K_2O	Cao	Fe_2O_3	MnO_2	TiO_2	CuO	NiO	Cr_2O_3
RSA	98.6	0.23	0.686	0.28	0.042	0.08	0.05	0.01	0.011

Table (2): Chemical composition, density (ρ) and molar volume (Vm) of the prepared BSiBi glasses (mol. %).

Sample	mol%				ρ (g/cm^3) ± 0.082	Vm (cm^3/mol) ± 0.075
	Bi_2O_3	B_2O_3	Na_2O	SiO_2		
BSiBi00	0	14	30	56	2.373	34.867
BSiBi05	5	13	30	52	2.825	36.251
BSiBi10	10	12	30	48	3.177	38.423
BSiBi15	15	11	30	44	3.353	40.105
BSiBi20	20	10	30	40	4.076	39.595

The X-ray diffraction (XRD) is an analytical method established on the diffraction of X-rays to identify the structure of materials, whether the material is non-crystalline or amorphous phase. XRD characteristic was demonstrated for our prepared BSiBi glass samples with a wide hollow band at 2θ around (20-35), as shown in Figure (1) which indicates no sharp peaks and the amorphous status of the glass.

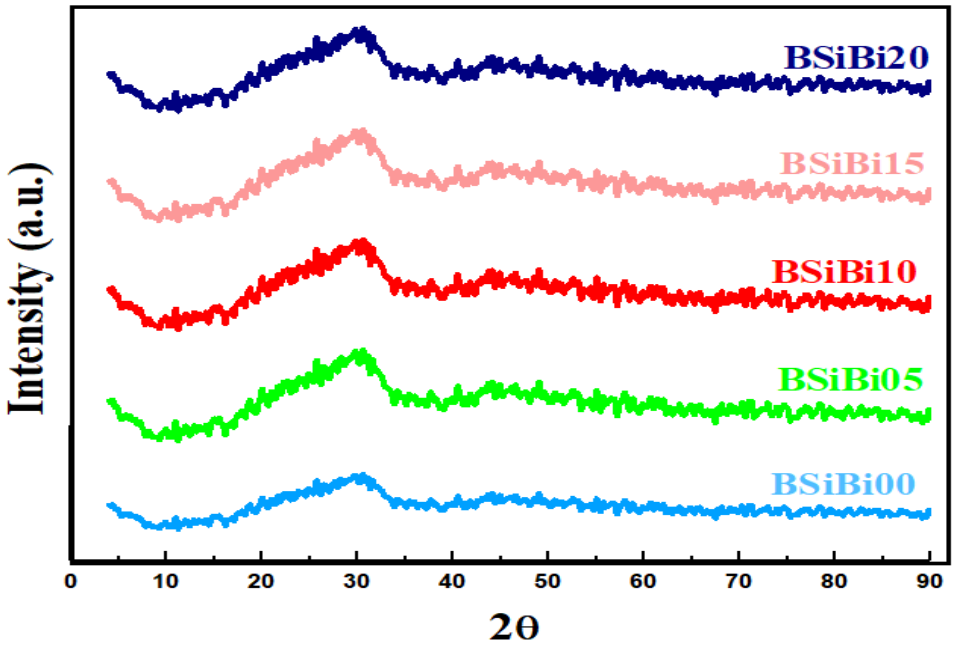

Fig. 1. The XRD spectrum of the arranged BSiBi glasses

The LAC is a crucial parameter that accounts for every possible photon interaction cross-section that occurred with every element in the glass composition. Table (3) and Figure (2) show the theoretically predicted values using the WINXCOM program for the different glasses composition at different incident photon energy up to ~ 15 MeV. From figure (2), it can be shown that the LAC values present the same behavior for all investigated glasses except for BSiBi00. Due to the different content of Bi atom in those glasses, the LAC values increased as the Bi_2O_3 contents increased. Accordingly, LAC values follow the order BSiBi20> BSiBi15> BSiBi10> BSiBi05. At the low energy region (81–200 keV), the abrupt increase in the LAC values was followed by a very fast decrease at 90 keV. The effect is related to the occurrence of the K-absorption edge of the Bi content. The (K-edge) is a sudden rise in the photoelectric absorption of x-ray photons reported at an energy level just beyond the binding energy of the Bi absorbing atom's k-shell electrons. At an intermediate energy region, the effect of photoelectric interaction decreases, and the Compton scatting dominate. At high energy region > 1.02 MeV, the pair production cross-section dominate, while the difference in the LAC values becomes less important as indicated in the figure.

Table (3):The theoretical linear attenuation coefficients at different photon energy for varied Bi2O3 concentrations.

Energy (MeV)	LAC				
	BSiBi00	BSiBi05	BSiBi10	BSiBi15	BSiBi20
1.50E-02	10.827	92.657	158.515	216.833	283.588
2.00E-02	4.784	68.440	119.689	165.000	216.657
3.00E-02	1.695	24.112	42.159	58.116	76.308
4.00E-02	0.944	11.565	20.116	27.679	36.309
5.00E-02	0.672	6.608	11.386	15.615	20.449
6.00E-02	0.546	4.240	7.212	9.846	12.863
8.00E-02	0.435	2.196	3.612	4.871	6.322
1.00E-01	0.385	4.463	7.745	10.648	13.963
2.00E-01	0.293	1.002	1.572	2.080	2.674
3.00E-01	0.251	0.522	0.739	0.936	1.173
4.00E-01	0.224	0.371	0.488	0.596	0.730
5.00E-01	0.205	0.301	0.377	0.448	0.541
6.00E-01	0.189	0.260	0.315	0.368	0.439
7.79E-01	0.168	0.216	0.254	0.290	0.342
8.00E-01	0.166	0.212	0.249	0.284	0.334
9.64E-01	0.152	0.188	0.217	0.246	0.286
1.00E+00	0.149	0.184	0.212	0.239	0.278
2.00E+00	0.105	0.126	0.143	0.160	0.186
3.00E+00	0.085	0.106	0.123	0.139	0.163
4.00E+00	0.074	0.096	0.113	0.130	0.154
5.00E+00	0.067	0.090	0.109	0.126	0.150
6.00E+00	0.062	0.087	0.106	0.125	0.150
8.00E+00	0.055	0.083	0.105	0.126	0.152
1.00E+01	0.052	0.082	0.106	0.128	0.157
1.50E+01	0.048	0.083	0.112	0.138	0.170

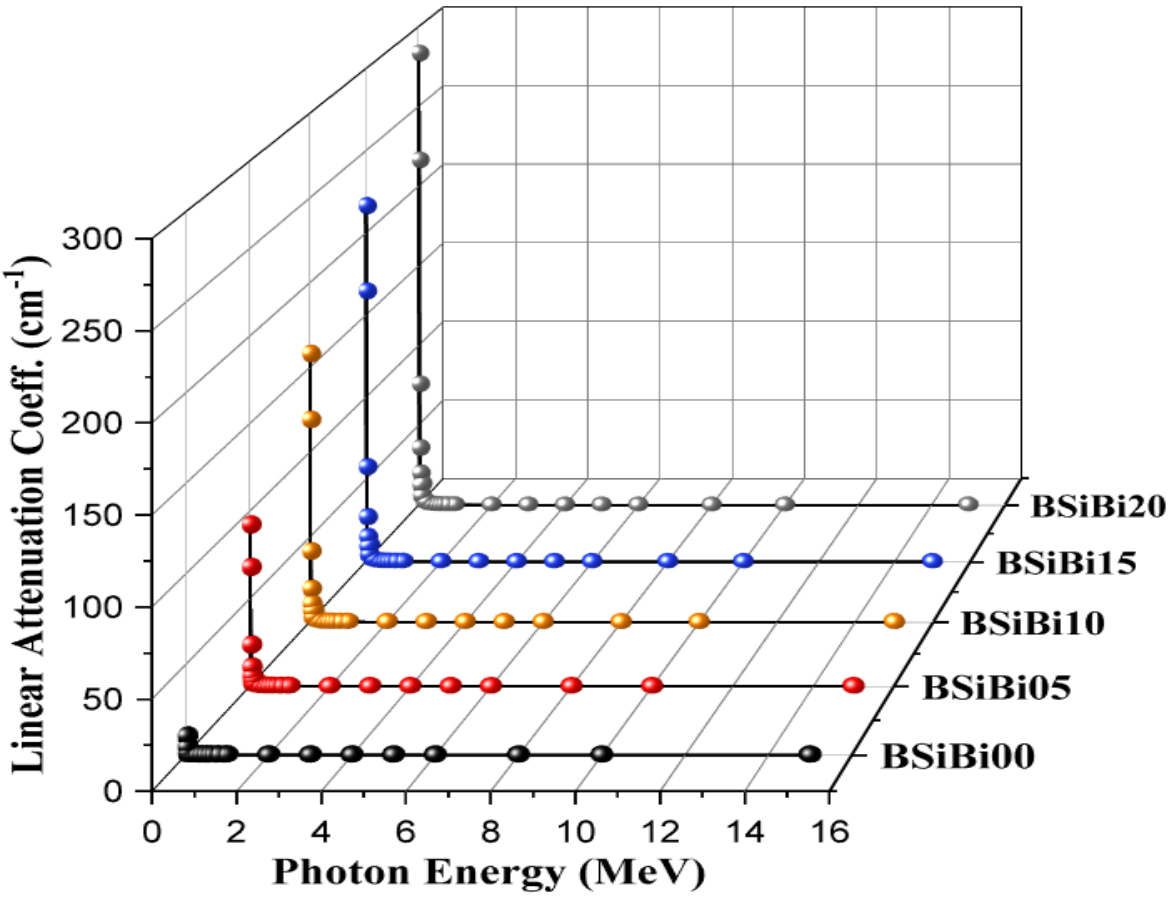

Fig. 2. The theoretical linear attenuation coefficients as a function of gamma ray energy for varied Bi2O3 concentrations.

The HVL and the MFP are the most widely utilized quantitative parameters that characterize the ability of specific energetic photons to permeate the selected shielding materials. As aforementioned, HVL is the thickness of the shielding material required to lower photon beam intensity to half of its starting value, and MFP is the mean distance traveled between two successive photon interactions within the material. Therefore, the shorter the HVL and MFP, the better is the material shielding capabilities. For our prepared glasses, values of the HVL and MFP are calculated and presented in figure (3). It is observed that with the increase of glass density (ρ) as well as Bi_2O_3 contents in the studied glasses, the values of those two parameters are decreased. The increase in MAC with increased Bi_2O_3 concentration can explain the decrease in HVL and MFP. As a result, the BSiBi20 glass has the lowest HVL and MFP, indicating higher attenuation ability. The current results present good signs that our prepared Bi-borate-RSA glasses can be considered a good radiation protective material, mainly for low-energy gamma-rays.

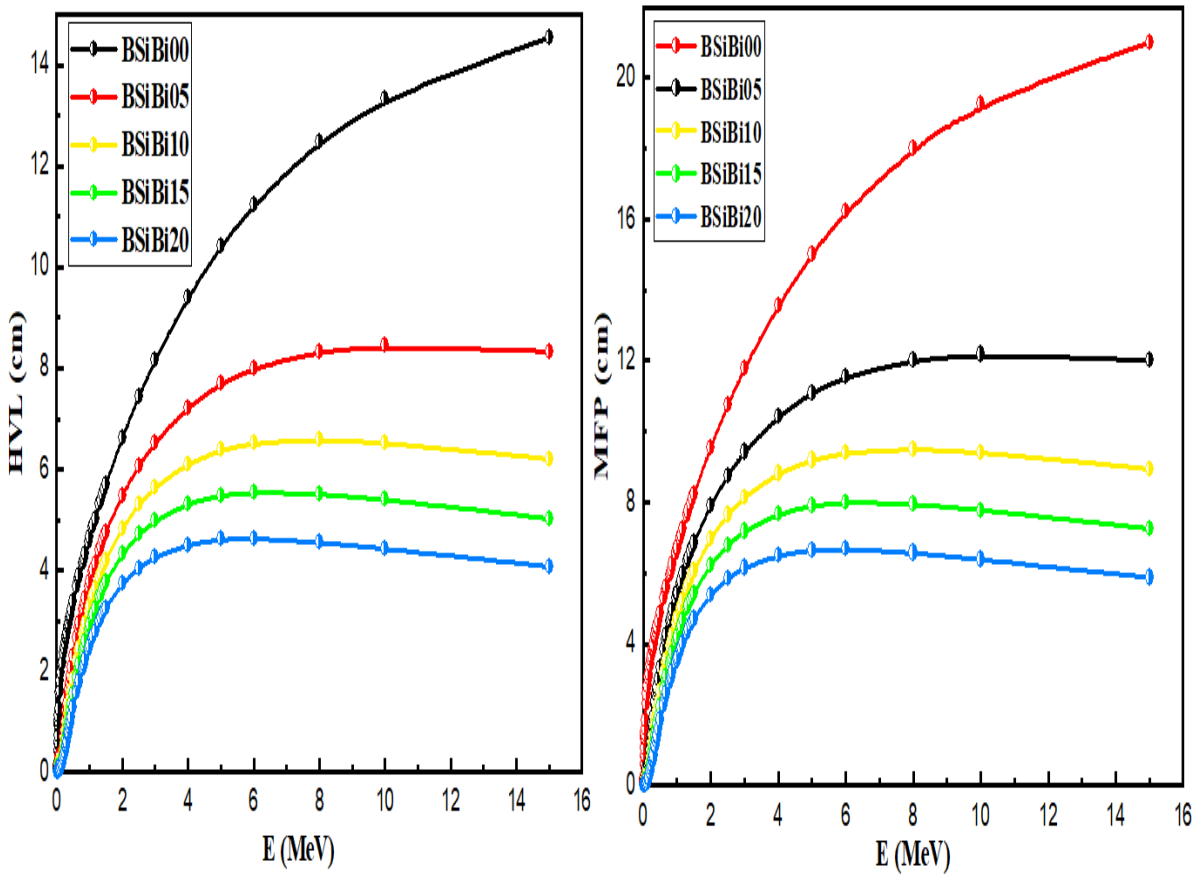

Fig. 3. HVL and MFP values of BSiBi glass are expressed as a function of gamma-ray photon energies.

Table (4) and Figure (4) depicts the variation of Z_{eff} as a function of photon energy, showing that the Z_{eff} values obtained theoretically using WINXCOM at various gamma-ray energies. Initially, similar behaviors to LAC were observed, where a fast increase in the Z_{eff} values (80–90 keV) was followed by a very fast decrease (90 - 300 keV) and then slowly decreased up to 1200 keV. In the low energy region, the photoelectric effect is the dominance where there was a fast increase; the effect is related to the occurrence of the K-absorption edge of the Bi atoms (90 keV). The following rapid decrees were observed at intermediate energies due to the diminishing of the photoelectric effect and where Compton scattering interaction began to act and Z_{eff} values decreases up to 1200 keV. The BSiBi20 > BSiBi15 > BSiBi10 > BSiBi05 series glasses have the highest Z_{eff} values because of the increased abundance of Bi_2O_3, contents the addition of SiO_2 to the BSiBi glass systems has also increased the Z_{eff} values.

Table (4):The theoretical effective atomic number at different photon energy for varied Bi_2O_3 concentrations.

Energy (MeV)	Z_{eff}				
	BSiBi00	BSiBi05	BSiBi10	BSiBi15	BSiBi20
1.50E-02	11.52	50.82	62.66	68.36	71.72
2.00E-02	11.40	59.98	69.58	73.69	75.97
3.00E-02	10.98	59.08	68.92	73.16	75.52
4.00E-02	10.51	55.46	66.23	71.07	73.82
5.00E-02	10.14	50.41	62.21	67.86	71.16
6.00E-02	9.89	44.98	57.49	63.92	67.83

8.00E-02	9.62	35.37	47.90	55.31	60.20
1.00E-01	9.49	52.01	63.47	68.80	71.88
2.00E-01	9.35	27.18	38.16	45.60	50.98
3.00E-01	9.33	18.89	26.33	32.28	37.15
4.00E-01	9.33	15.76	21.21	25.90	29.96
5.00E-01	9.32	14.30	18.69	22.60	26.10
6.00E-01	9.32	13.52	17.30	20.72	23.84
7.79E-01	9.32	12.79	15.98	18.92	21.64
8.00E-01	9.32	12.73	15.87	18.78	21.47
9.64E-01	9.32	12.41	15.28	17.96	20.46
1.00E+00	9.32	12.36	15.19	17.83	20.30
2.00E+00	9.33	12.13	14.76	17.23	19.55
3.00E+00	9.35	12.52	15.46	18.20	20.75
4.00E+00	9.37	12.98	16.30	19.34	22.15
5.00E+00	9.40	13.46	17.14	20.48	23.54
6.00E+00	9.42	13.92	17.94	21.56	24.84
8.00E+00	9.47	14.76	19.40	23.49	27.14
1.00E+01	9.52	15.50	20.64	25.12	29.04
1.50E+01	9.60	16.95	23.04	28.17	32.55

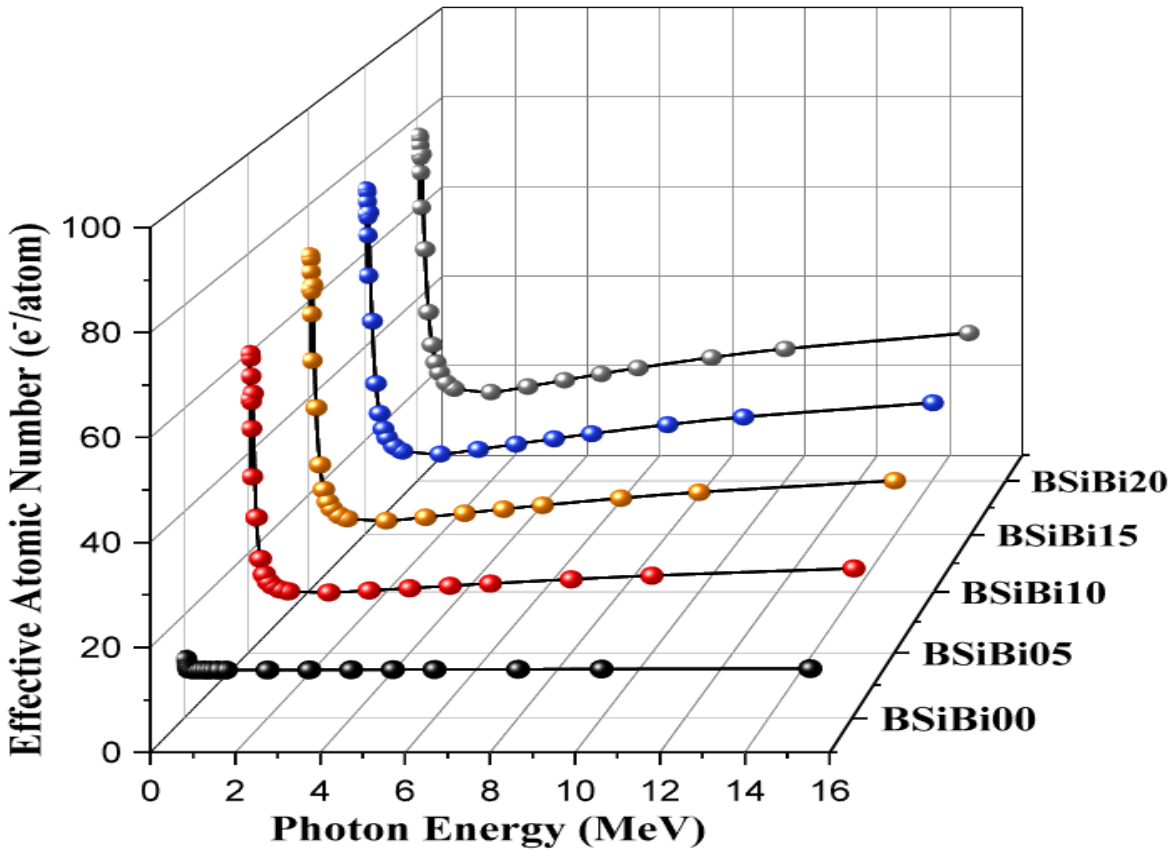

Fig. 4. The theoretical values of the Z_{eff} as a function of gamma ray energy for varied Bi_2O_3 concentrations.

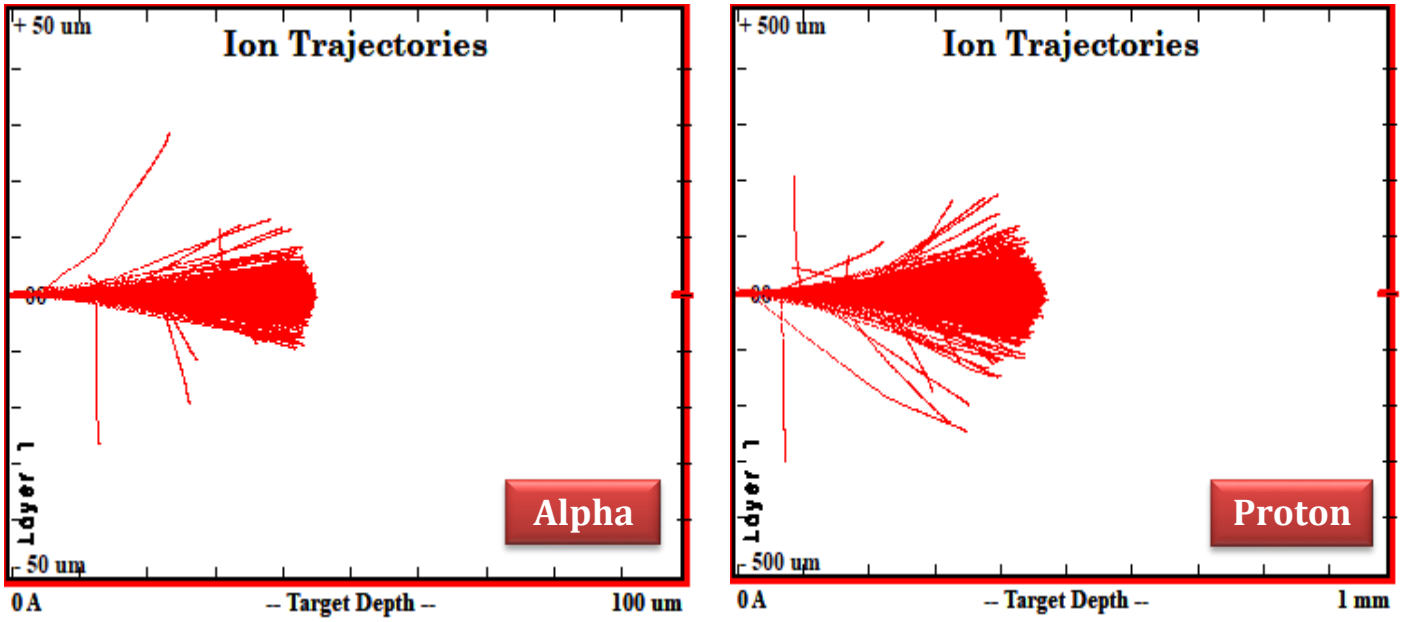

Fig. 5. SRIM simulation results of alpha and proton interaction with bismuth borate-RSA glass sample with (20% mol Bi_2O_3), the ion tracks are shown as red dots.

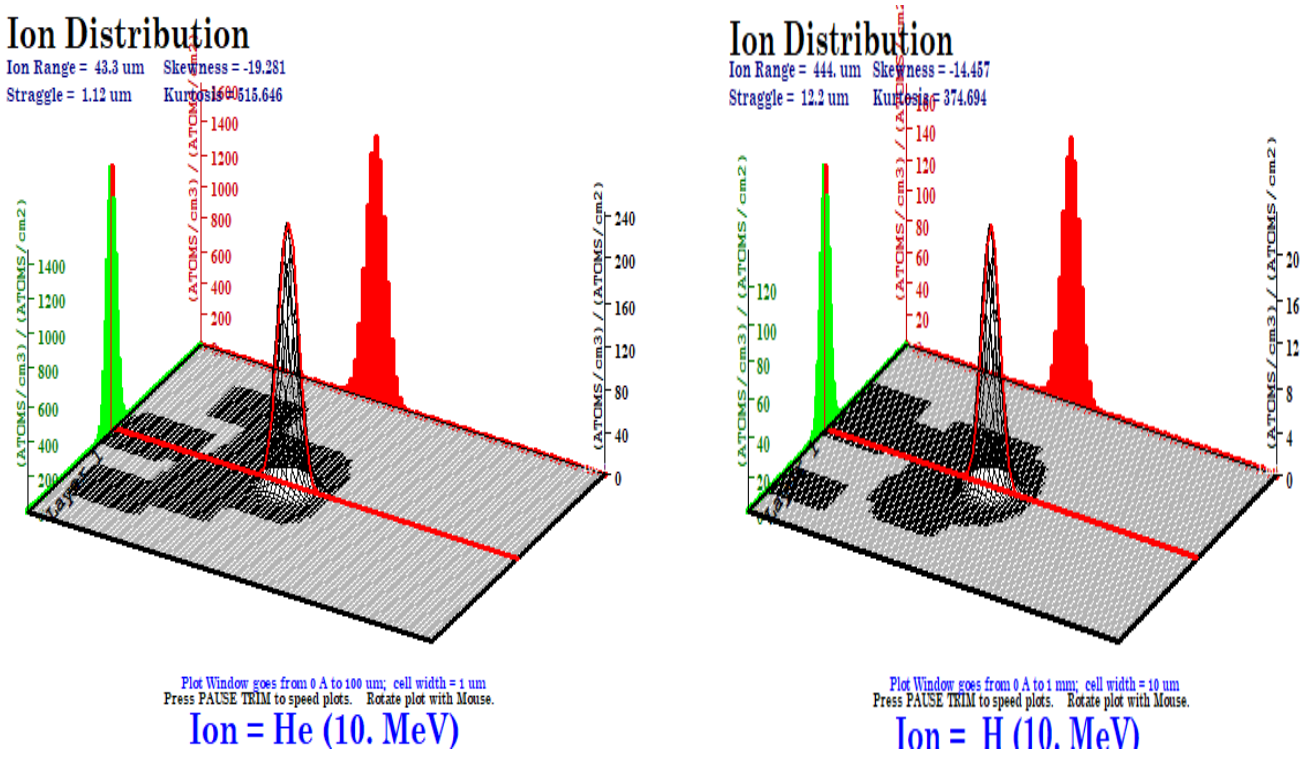

Fig. 6. 3D ion distribution image after interaction of alpha and proton with bismuth borate-RSA glass sample with (20% mol Bi_2O_3).

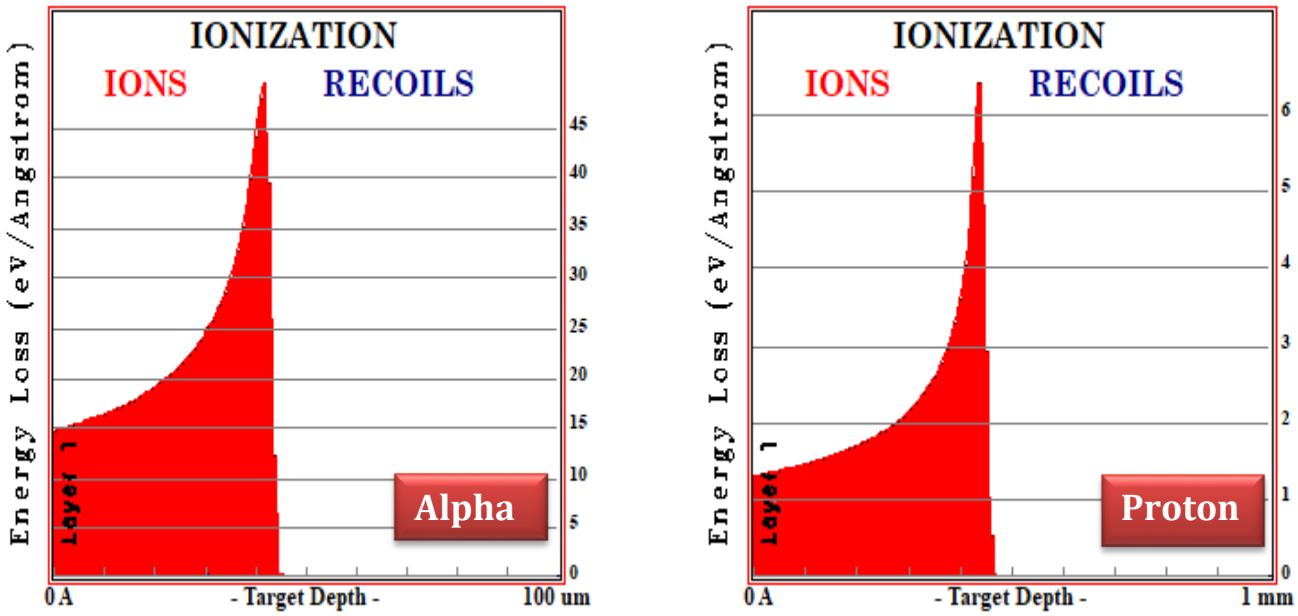

Fig. 7. a TRIM output results of the energy transfer to ionization as a result of implanted alpha and proton with recoil atoms.

The results of the SRIM-TRIM Simulation code of the interaction of 10 MeV alpha and proton with (0.20% Bi_2O_3) are presented in Figures (5,6,7) for more understand the interaction of alpha and proton with the target, the diffusion of alpha into the depth of 0.1 mm and proton into the depth of 1mm is obtained. Figure [5] demonstrates that recoil atoms framed the path, forming a path of the ions. The distribution of alpha and proton after arresting the bombardment is recorded range of 0.43mm for alpha and 4.4 mm for proton, as shown in Figure [6]. Figure [7] presents the ionization curve, which was also found from the simulation study. It should be noted that the figures display a strong ionization effect of the recoil atoms in the target. You can also notes that the losses of ion energy to the target electrons will cause board damage, where the charges may cause cracking and delamination.

IV. Conclusion

This paper gives an overview of recent eco-friendly bismuth borate-RSA glasses based on the silica from rice straw ash as a shield for cosmic radiation. In general, cosmic radiation can be subdivided into primary cosmic rays consists of protons and alpha particles and secondary cosmic rays, also including photons. Our developed glass has formula of (70-x) [$80SiO_2 – 20B_2O_3$] – $30Na_2O$ – x Bi_2O_3, where x:($0 \leq x \leq 20$). By using XRD, the non-crystalline nature of the glass samples is attributed. The theoretical shielding parameters have been study using WINXCOM software. The LAC and Z_{eff} values increased with the increase of the concentration of Bi_2O_3, whereas the HVL and MFP values decrease. Also, good charged particle shielding ability is observed. The results showed that among the produced glasses, the glass with 20 mol% Bi_2O_3 and 40 mol% SiO_2 is the best effective shield. Finally, it can be concluded that increasing content of Bi_2O_3 in the glass effected gamma, proton, and alpha particle shielding performance in an increasing direction of investigated glass samples. In the end, we recommend using our eco-friendly glass as cosmic ray protection to facilitate the invasion of space and to protect electronic devices from the distortion of radiation exposure.

REFERENCES

Almisned, G., Tekin, H.O., Kavaz, E., Bilal, G., Issa, S.M., Zakaly, H.H., Ene, A., 2021: Gamma, fast neutron, proton, and alpha shielding properties of borate glasses: a closer look on lead (II) oxide and bismuth (III) oxide reinforcement. Appl. Sci. 11, 6837.

Askin, A., 2020: Evaluation of the gamma and neutron shielding properties of 64TeO2 + 15ZnO + (20 − x)CdO + xBaO + 1V2O5 glass system using Geant4 simulation and Phy-X database software. Pramana - J. Phys. 94–97.

CENGI˙Za, G.B., ÇAGLAR, I., 2020: Assessment of mass attenuation coefficient, effective atomic number and electron density of some aluminum alloys. Bilgici Cengiz & Çaglar/Cauc. ˇ J. Science 7 (2), 109–122.

Kaewkhao, J., Laopaiboon, J., Chewpraditkul, W., 2008: Determination of effective atomic numbers and effective electron densities of Cu/Zn alloy. J. Quant. Spectrosc. Radiat. Transf. 109, 1260–1265.

Kassem, Said M., Ahmed, G.S.M., Rashad, A.M., Salem, S.M., Ebraheem, S., Mostafa, A. G., 2021: An investigation of the nuclear shielding effectiveness of some transparent glasses manufactured from natural quartz doped lead cations. Nucl. Eng. Technol. 53, 2025–2037.

Kaur, K., Singh, K.J., Anand, V., 2016: Structural properties of Bi2O3–B2O3–SiO2–Na2O glasses for gamma ray shielding applications. Radiat. Phys. Chem. 120, 63–72.

Ruengsri, S., Insiripong, S., Sangwaranatee, N., Kaewkhao, J., 2015: Development of barium borosilicate glasses for radiation shielding materials using rice husk ash as a silica source. Prog. Nucl. Energy 83, 99–104.

Sayyed, M.I., 2016a: Bismuth modified shielding properties of zinc boro-tellurite glasses. J. Alloys Compd. 688, 111–117.

Sayyed, M.I., 2016b: Investigations of gamma ray and fast neutron shielding properties of tellurite glasses with different oxide compositions. Can. J. Phys. 94, 1133–1137.

Sayyed, M.I., Lakshminarayana, G., Dong, M.G., Ersundu, M.Ç., Ersundu, A.E., Kityk, I. V., 2018a: Investigation on gamma and neutron radiation shielding parameters for BaO/SrO–Bi2O3–B2O3 glasses. Radiat. Phys. Chem. 145, 26–33.

Sayyed, M.I., Akman, F., Turan, V., Araz, A., 2018b: Evaluation of radiation absorption capacity of some soil samples. Radiochim. Acta 107 (1), 83–93.

Sayyed, M.I., Kaky, K.M., S¸ akar, E., Akbaba, U., Takie, M.M., Agar, O., 2019: Gamma radiation shielding investigations for selected germanate glasses. J. Non-Cryst. Solids 512, 33–40.

Sayyed, M.I., Olarinoye, O.I., Elsafi, M., 2021: Assessment of gamma-radiation attenuation characteristics of Bi2O3–B2O3–SiO2–Na2O glasses using Geant4 simulation code. Eur. Phys. J. A 136, 535.

Singh, H., Singh, K., Gerward, L., Sahota, H.S., Nathuram, R., 2003: ZnO-PbO B2O3 glasses as gamma-ray shielding materials. Nucl. Instrum. Methods Phys. Res. Sect. B Beam Interact. Mater. Atoms 207, 257–262.

Tuscharoen, S., Kaewkhao, J., Limsuwan, P., Chewpraditkul, W., 2012: Structural, optical and radiation shielding properties of BaO-B2O3-rice husk ash glasses. Procedia Eng. 32, 734–739.

Vermani, Y.K., Singh, T., 2021: Numerical investigation on photon energy absorption parameters for some Bi–Sn–Zn alloys in wide energy region. Pramana - J. Phys. 95, 112.